energies

MDPI

Review

Solid Oxide Electrolysis, Co-Electrolysis, and Methanation Fundamentals of Performance and History

Katsiaryna Martsinchyk, Aliaksandr Martsinchyk and Jaroslaw Milewski *

Institute of Heat Engineering, Faculty of Power and Aeronautical Engineering, Warsaw University of Technology, 21/25 Nowowiejska str., 00-665 Warsaw, Poland; katsiarina.martsinchyk.dokt@pw.edu.pl (K.M.); aliaksandr.martsinchyk.dokt@pw.edu.pl (A.M.)
* Correspondence: jaroslaw.milewski@pw.edu.pl

Abstract: This manuscript discusses the advancements and historical development of solid oxide electrolysis (SOE), co-electrolysis, and methanation technologies, addressing the performance fundamentals and system integration challenges in the context of the EU's 2050 climate neutrality goals. SOE technologies, characterized by their high efficiencies and ability to operate at elevated temperatures, offer significant advantages in hydrogen production and power generation. Co-electrolysis of steam and carbon dioxide in SOEs provides a promising pathway for syngas production, leveraging carbon capture and utilization strategies to mitigate carbon emissions. Additionally, catalytic methanation processes described within facilitate the synthesis of methane from carbon oxides and hydrogen, which could be integral to renewable energy storage and grid-balancing solutions. Historical analysis provides insights into the evolution of these technologies from early experiments to modern applications, including their role in space programmes and potential for industrial scale-up. The current state of research and commercialization, highlighted through various system designs and operational enhancements, suggests that SOEs are crucial for sustainable energy transformations, underscoring the necessity for continued innovation and deployment in relevant sectors.

Keywords: solid oxide electrolysis; co-electrolysis; methanation; hydrogen production; carbon capture and utilization; syngas; renewable energy; high temperature electrolysis; catalytic reactors; energy transition

Citation: Martsinchyk, K.; Martsinchyk, A.; Milewski, J. Solid Oxide Electrolysis, Co-Electrolysis, and Methanation Fundamentals of Performance and History. *Energies* **2024**, *17*, 6486. https://doi.org/10.3390/en17246486

Academic Editor: Giorgio Vilardi

Received: 2 November 2024
Revised: 9 December 2024
Accepted: 10 December 2024
Published: 23 December 2024

Copyright: © 2024 by the authors. Licensee MDPI, Basel, Switzerland. This article is an open access article distributed under the terms and conditions of the Creative Commons Attribution (CC BY) license (https://creativecommons.org/licenses/by/4.0/).

1. Introduction

"The EU aims to be climate-neutral by 2050—an economy with net-zero greenhouse gas emissions. This objective is at the heart of the European Green Deal and in line with the EU's commitment to global climate action under the Paris Agreement." (https://climate.ec.europa.eu/eu-action/climate-strategies-targets/2050-long-term-strategy_en (accessed on 27 September 2024), 2021).

Global energy consumption was increasing with the world's development (Figure 1a). Consequently, the emissions were also growing because of the primary energy source: fossil fuels (Figure 1b). Due to global worldwide challenges, like the world economic crisis in 2008–2099 and the COVID-19 pandemic in 2020, energy consumption fell (Figure 1), causing fewer emissions. But the global reduction to meet the goals of the Green Deal [1] and REPowerEU [2] is achievable only by the development and change of energy production technology.

To reach the goals, systems of carbon capture and storage (CCS), carbon capture and utilization (CCU), and carbon recycling and reuse (CRR) [3] should be implemented on a large scale, and the share of renewable energy systems (RESs) should continuously grow.

The energy generation from RESs has been rapidly increasing since 2006 (Figure 2).

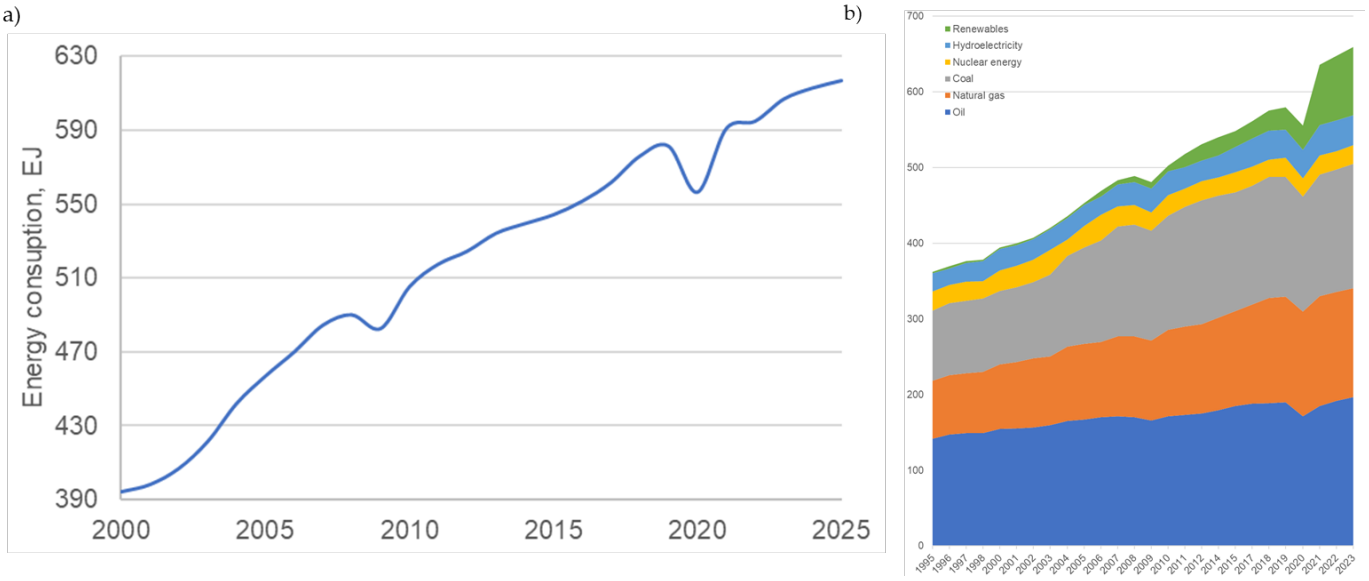


Figure 1. Global energy consumption (**a**) in general and (**b**) by source (source: BP Energy Outlook 2023–2024).

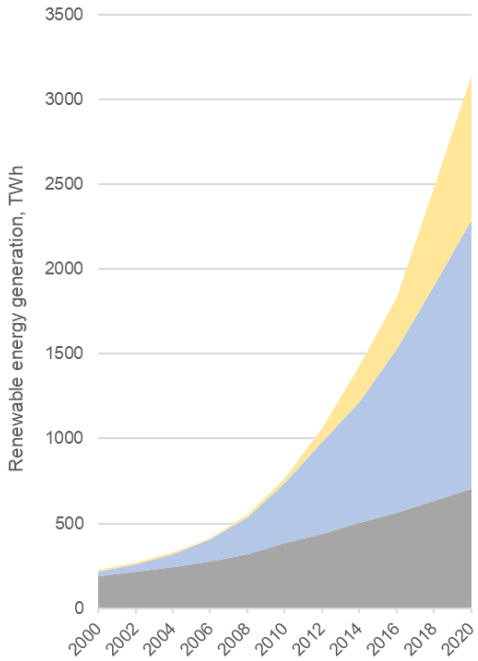


Figure 2. Global renewable energy generation by source (source: BP Statistical Review of World Energy 2021, 70th edition).

Such rapid development and implementation of renewables, mainly solar and wind, has a major issue: the risk of imbalance between demand and production due to the intermittent character of renewables, which causes the necessity to implement technologies to use the excess electricity [4].

To tackle the issues of the Green Deal, REPowerEU plan, and RESs' intermittent character, electrolysis technology could be crucial.

Electrolysis is an electrochemical method that splits water into hydrogen and oxygen by using electrical energy, such as surplus power generated from renewable energy sources (RESs). That process can take place in three main types of electrolysers: alkaline, proton exchange membrane (PEM), or solid oxide electrolysers. The SOE technology is

one of the most efficient, with low energy demand (36–42 kWh/kg H_2 [5,6]), high current/power density, and high gas purity.

The climate and decarbonization issues have increased interest in developing carbon capture, utilization, storage, and reuse technologies. Currently, the most developed and mainly used carbon capture technology is amine scrubbing. And the prospective further carbon utilization is the electrochemical conversion of CO_2 or CO_2 together with H_2O [7–12].

The electrolysis of H_2O and/or CO_2 in SOE was firstly introduced by NASA in the late 1960s [13,14]. But attention only returned to that topic in the 1980s by [15–17], where the performance of the solid oxide electrolyser producing the hydrogen was analysed. Further, in the early 2000s, NASA investigated the methods of oxygen production via CO_2 electrolysis [18,19], which brought the topic of H_2O and/or CO_2 to a high level of interest. Ebbesen [7,9,20–22] has provided numerous studies on the effective simultaneous reduction of CO_2 and H_2O in 2009–2012. The latest investigations in that field are mainly concentrated on material improvement [11], optimization of the system layout [23], and performance experiments [10,24].

2. SOE Fundamentals of Performance

The electrolyser considered in this study is the solid oxide electrolyser (SOE). Due to the usage of ceramic electrolyte, this type of electrolyser runs at high temperatures between 650 °C and 900 °C. The layers of a solid oxide cell are the cathode, the anode, and the electrolyte. YSZ (ZrO_2 doped with 8 mol% Y_2O_3) for the electrolyte, nickel for the fuel electrode, and LSM (lanthanum strontium manganate) for the oxygen electrode are the most prevalent materials for SOE. Recent research results show that the materials face degradation challenges that impact their operational lifespan. Studies have reported degradation rates of approximately 0.75% to 1.4% voltage loss per 1000 h for cells operating between 750 °C and 850 °C. To mitigate these issues, advancements include the development of co-doped zirconia electrolytes, which enhance ionic conductivity and reduce degradation. Additionally, incorporating gadolinium-doped ceria (GDC) interlayers between the electrolyte and electrodes has been shown to improve chemical compatibility and suppress interfacial reactions, thereby extending cell longevity. Improved kinetics, thermodynamics favouring the utilization of internal heat at higher temperatures, and steam conversion all contribute to enhanced performance and allow for the attainment of high efficiencies in the 80–90% range [25–29].

The water steam is utilized and converted into hydrogen and oxygen in the SOE process. Steam enters the porous fuel electrode (cathode) and proceeds to the cathode–electrolyte interface, where it is reduced to H_2 and oxygen ions. Hydrogen gas diffuses back via the cathode, whereas oxygen ions $O^=$ are conducted through the electrolyte. Oxygen ions are oxidized to generate pure oxygen gas at the contact between the electrolyte and anode. Figure 3 presents the described process. The reactions that occur on the cathode side and the anode side are given in Equations (1) and (2), respectively.

$$H_2O + 2e^- \rightarrow H_2 + O^= \quad (1)$$

$$O^= \rightarrow \frac{1}{2}O_2 + 2e^- \quad (2)$$

When comparing solid oxide electrolysis, co-electrolysis, and proton exchange membrane electrolysis technologies, it is essential to evaluate their differences in efficiency, cost, and scalability. SOE systems are highly efficient due to their operation at temperatures between 650 and 900 °C, which enhances their thermodynamic performance. This high operational temperature allows for the utilization of waste heat streams, boosting overall system efficiency to between 80 and 90%. Conversely, PEM electrolysers operate at lower temperatures (up to 80 °C) and typically achieve efficiencies of around 60–70%, although they benefit from rapid response times and can effectively balance the intermittent nature of renewable energy sources like wind and solar.

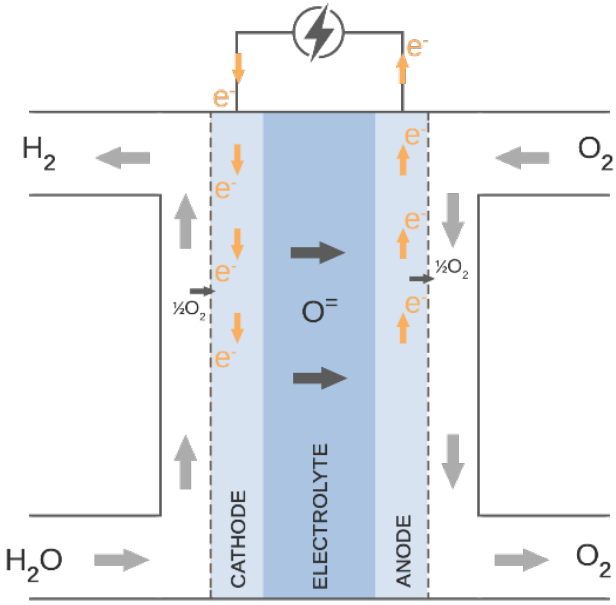


Figure 3. Electrolysis process.

In terms of cost, SOE technologies generally require higher capital investment because they need materials that can withstand high temperatures, impacting both the initial setup and ongoing maintenance costs. PEM systems, while also reliant on costly catalysts such as platinum and iridium, avoid the need for the specialized materials required for high-temperature operations, making them less expensive in this regard, although the cost of catalysts remains a significant factor.

Scalability is another critical factor. SOE technologies face challenges in scaling due to the demands of high-temperature operation and the need for durable materials that maintain performance at larger scales. They are better suited for integration with industrial processes that can use the heat and hydrogen produced. PEM electrolysers, however, are more adaptable to various scales and can quickly adjust to power availability, making them ideal for fluctuating power supplies from renewable sources.

Choosing between SOE and PEM technologies often depends on specific needs such as the availability of heat sources, the capacity for capital investment, and the desired integration with other energy systems. While SOE and co-electrolysis provide superior efficiency with proper heat integration, PEM electrolysers offer more flexibility and scalability under varying operational conditions.

3. Co-SOE Fundamentals of Performance

The carbon-neutral, zero-emission, synthetic fuel can be produced via high-temperature co-electrolysis of H_2O and CO_2. Currently, there are two technologies able to perform co-electrolysis as a one-step process: solid oxide co-electrolysis and molten carbonate electrolysis [30]. Captured CO_2 could be delivered with the steam to the solid oxide electrolyser and reduced to the H_2 + CO gas mixture (syngas) utilizing electric power, e.g., from renewable energy sources. The schematic diagram of the process of co-electrolysis operation is shown in Figure 4. The overall reaction occurring inside the co-electrolyser is given in Equation (3).

$$H_2O + CO_2 \rightarrow H_2 + CO + O_2 \quad (3)$$

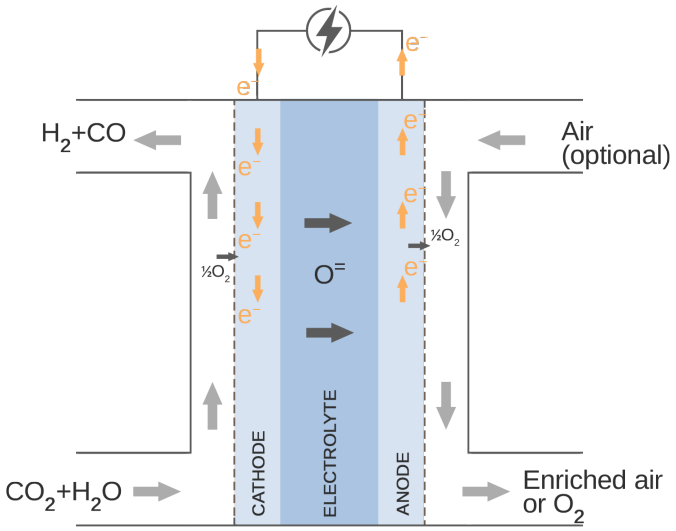


Figure 4. Co-electrolysis process.

As presented in Figure 4, the carbon dioxide and steam are supplied to the cathode side of the co-electrolyser. At the cathode–electrolyte interface, the H_2O and CO_2 are reduced to H_2 and CO, which diffuse back through the fuel electrode, and oxygen ions pass through the electrolyte and oxidize to oxygen or enrich the air supplied to the anode side of the electrolyser.

The electrochemical reactions of H_2O and CO_2 reduction on the cathode side are described in Equation (2) and (3). The oxidation reaction of the oxygen ions is given in Equations (4)–(6).

$$H_2O + 2e^- \rightarrow H_2 + O^= \quad (4)$$

$$CO_2 + 2e^- \rightarrow CO + O^= \quad (5)$$

$$O^= \rightarrow \frac{1}{2}O_2 + 2e^- \quad (6)$$

Depending on the operational temperature and catalyst used, syngas can be produced by electrochemical reduction of H_2O and CO_2 at a heterogeneous catalyst (e.g., nickel) or by means of electrochemical reduction of H_2O to H_2 followed by a homogeneous/heterogeneous [31–36] reverse water gas shift (RWGS) reaction [10,11], which occurs with a fast kinetic rate at the cathode side at high temperatures (above 720 °C [37]). The RWGS reaction is given by the following equation:

$$H_2 + CO_2 \leftrightarrow CO + H_2O \quad (7)$$

4. Methanation Reactor Fundamentals of Performance

Catalytic methanation, also known as the Sabatier reaction, involves the conversion of carbon oxides and hydrogen into methane. This reaction was first proposed and detailed by Paul Sabatier [38]. Various reactor designs are based on this principle, including the packed-bed Sabatier reactor, which is a type of heat exchanger, suggested by Sun D. and Simakov D. [39]. Other designs include the two-phase honeycomb reactor and the three-phase slurry bubble column reactor, both introduced by Held M. et al. [40].

Figure 5 illustrates a packed-bed Sabatier reactor of the heat exchanger type with cooling tubes containing flowing molten salt. According to Sun D. and Simakov D. [39], the proposed model presents a high CO_2 conversion rate, good thermal management, and flexibility in catalyst installation and usage.

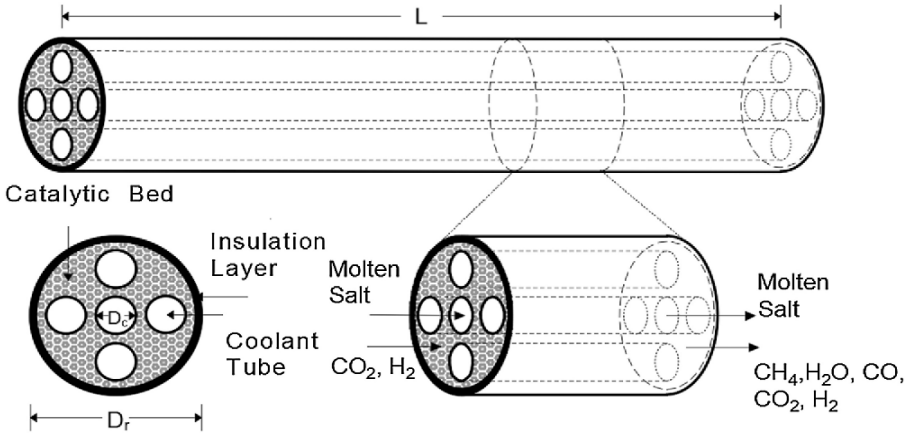


Figure 5. Packed-bed Sabatier reactor.

The honeycomb reactor is a two-phase structured fixed-bed reactor. It is a multitube reactor with parallel tubes for the metallic catalyst carriers. The conversion of CO_2 and H_2 to CH_4 occurs in the porous catalyst layer, and most of the reaction heat is released at the channel inlets [40].

A slurry bubble column reactor is a vertical cylinder in which three phases are in close contact: gaseous inlet (CO_2 and H_2) at the bottom of the column, the liquid product, and the solid catalyst. Using a specialized gas distributor at the bottom of the column, the gas phase is distributed into the liquid phase [41]. Heat management in that reactor type is presented by heat transfer fluid, which has a high heat capacity, allowing for effective heat transfer from the catalyst particles to the cooling medium in the cooling jacket [40].

A schematic drawing of the honeycomb reactor is shown in Figure 6a, and the slurry bubble reactor is presented in Figure 6b.

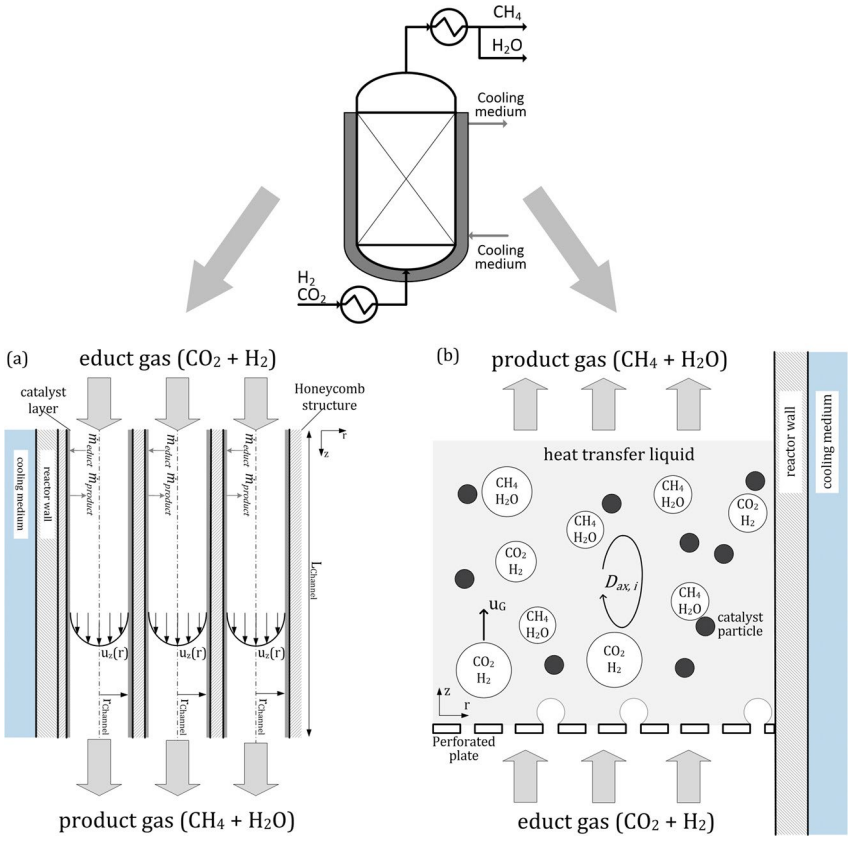


Figure 6. Methanation reactors: (**a**) honeycomb type, (**b**) slurry bubble column type [40].

The honeycomb methanation reactor provides high specific CH_4 production and excellent load flexibility. Comparing the two types of methanation reactors, the slurry bubble column reactor has a lower specific methane generation but a significantly better dynamic operation.

For the methanation process, catalysts based on Ni or Ru are required. Catalyst type, activity, and selectivity characteristics have the most influence on the process. Sabatier and Sendenders [38] discovered that nickel could catalyse the reaction between carbon oxides and hydrogen, which produces methane and water. For CO_2 methanation, nickel supported on various metal oxides is the most frequent form of catalyst. The primary benefits are high activity, excellent CH_4 selectivity, and low cost [42].

There are two prevalent processes for CO_2 methanation:

1. Without CO intermediate reaction.
2. With CO intermediate reaction.

The first approach for the direct conversion of carbon dioxide to methane was proposed by Medsforth S. [43] and is characterized by the conversion chain shown below:

$$CO_2 \rightarrow H_2C(OH)_2 \rightarrow CH_2O \rightarrow CH_3OH \rightarrow CH_2 \rightarrow CH_4$$

and further, that mechanism was developed by Pichler H. [44]. The proposed reactions of CO_2 methanation are presented in Equations (8)–(11).

$$CO_2 + 2H \rightarrow C(OH)_2 \quad (8)$$

$$C(OH)_2 + H \rightarrow CH_2O + H_2O \quad (9)$$

$$CH_2O + 2H \rightarrow CH_3OH \quad (10)$$

$$CH_3OH + 2H \rightarrow CH_4 + H_2O \quad (11)$$

The second type of conversion consists of the first CO_2 conversion to CO by the reversed water gas shift reaction (Equation (12)), followed by the conversion of CO to methane (Equations (13)–(16)). The reaction set, defined by Choe S.J. et al. [45], is presented below:

$$CO_2 + H_2 \rightarrow CO + H_2O \quad (12)$$

$$CO + H_2 \rightarrow C + H_2O \quad (13)$$

$$C + H \rightarrow CH \quad (14)$$

$$CH + H \rightarrow CH_2 \quad (15)$$

$$CH_2 + 2H \rightarrow CH_4 \quad (16)$$

The equilibrium conditions for the methanation process are highly dependent on the reaction's temperature and pressure. Due to the exothermic character of the reaction, as seen in Figure 7 [46,47], the methane generation rate generally decreases with increasing temperature and increases with increasing pressure. To maintain a high degree of conversion under ambient pressure, the temperature must be below 400 °C, but when pressure is increased, the practical temperature range expands (Figure 7). Numerous studies have analysed the optimal operating parameters for the methanation process. For example, one study [48] identifies the ideal conditions as a pressure range of 1 to 30 bar and a temperature between 200 °C and 300 °C. Another investigation [46] suggests that for systems combining solid oxide electrolysis (SOE) and a methanation reactor, the optimal parameters for effective CO_2 utilization are around 40–60 bar and temperatures between 170 °C and 210 °C. Additionally, from a techno-economic perspective, the optimal pressure is found to be 20–30 bar with similar temperature conditions [49].

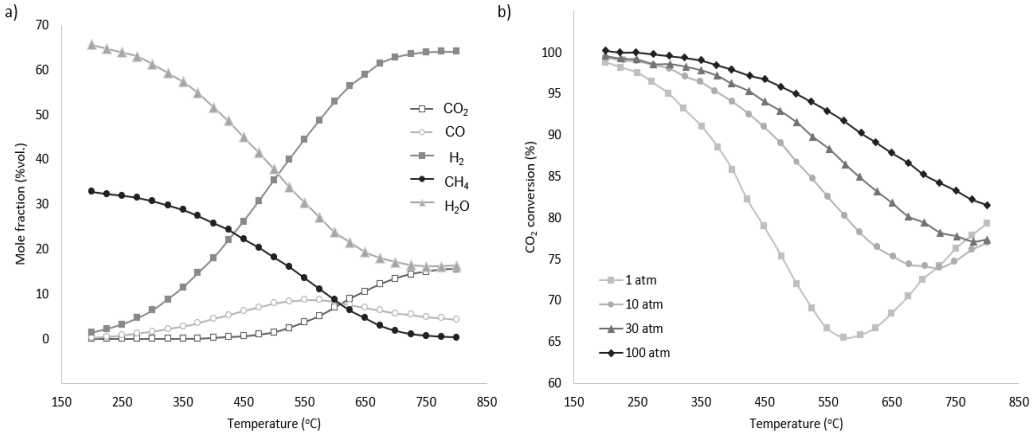


Figure 7. (**a**) Equilibrium product factor for methanation at 1 atm. (**b**) Pressure influence on CO_2 conversion for different temperatures [49].

Methanation reactors play a pivotal role in the production of synthetic methane, with different designs tailored to specific applications. The manuscript introduced three prominent reactor types. For industrial-scale methane production, packed-bed reactors are preferred due to their efficiency and thermal stability. In contrast, honeycomb reactors are better suited for grid-balancing applications, given their high productivity and adaptability to load variations. Slurry bubble column reactors, while less efficient in methane output, offer operational flexibility that aligns well with renewable energy systems.

The comparison (Table 1) underscores the need for careful reactor selection based on the intended application, highlighting the trade-offs between efficiency, operational challenges, and flexibility. Further research to optimize these designs for specific scenarios can enhance their utility across diverse energy systems.

Table 1. Comparison of three methanation reactor technologies.

Packed Bed	Honeycomb	Slurry Bubble Column
This design, exemplified by the heat exchanger model, features high CO_2 conversion rates and effective thermal management. The inclusion of molten salt cooling tubes ensures steady heat dissipation, which is critical for the exothermic Sabatier reaction. Packed-bed reactors are well suited for industrial-scale methane production due to their high throughput and thermal stability, but they may face challenges with heat transfer limitations at larger scales and under dynamic load conditions.	This structured, fixed-bed design offers high CH_4 productivity and excellent load flexibility, making it a strong candidate for grid-balancing applications where rapid response to fluctuating energy inputs is required. However, maintaining uniform flow distribution and catalyst activity across the reactor channels can be challenging, particularly under varying operational loads.	This reactor excels in dynamic operation due to the intimate contact between gaseous reactants, liquid medium, and solid catalyst. Its high heat capacity, facilitated by the cooling jacket and heat transfer fluid, provides superior thermal management. However, it has lower specific methane generation compared to the other designs, limiting its efficiency for large-scale production. Its ability to adapt to intermittent power supply makes it particularly advantageous for renewable energy integration scenarios.

5. The Beginning of High-Temperature Electrolysis

The initial demonstration of water electrolysis was conducted in 1789 by Adriaan Paets van Troostwijk and Jan Rudolph Deiman, who used an electrostatic generator to create an electrostatic discharge between two gold electrodes submerged in water [50–52]. Subsequent improvements by Johann Wilhelm Ritter made use of Volta's battery technology to facilitate the separation of product gases [53]. Dmitry Lachinov, in 1888, introduced an industrial method for the synthesis of hydrogen and oxygen through electrolysis,

advocating for the use of alkaline solutions as electrolytes because they are less corrosive to iron electrodes than acidic solutions [54]. By 1902, more than 400 industrial water electrolysers were in use [55]. These early devices predominantly utilized aqueous alkaline solutions as their electrolytes. The technique of water electrolysis using a proton exchange membrane was first described in the 1960s by General Electric, originally developed to generate electricity for NASA's Gemini Space Program, and was subsequently adapted to electrolysis for oxygen production.

The main historical points of electrolysis technology development are summarized in Table 2.

Table 2. History of water electrolysis.

Date	Event/Innovation	Ref.
1789	Adriaan Paets van Troostwijk and Johan Rudolph Deiman utilized an electrostatic generator to create a discharge between two gold electrodes submerged in water.	[50–52,56]
1800	Independently, William Nicholson, Anthony Carlisle, and Johann Wilhelm Ritter successfully demonstrated the fundamental principle of water electrolysis.	[56–58]
1834	Michael Faraday refined and established the foundational laws governing the electrolysis process.	[56,59]
1866	August Wilhelm von Hofmann designed a voltameter capable of electrolysing water and quantifying the resultant products.	[56,60–63]
1888	Dmitry Lachinov pioneered the industrial method for producing hydrogen and oxygen through electrolysis.	[54,56]
1899	Dr. O. Schmidt introduced the first industrial bipolar electrolyser, utilizing the filter press design and produced by Oerlikon.	[56]
1924	Jacob Emil Noeggerath designed the inaugural electrolyser capable of operating under high pressures (up to 100 bars) and secured a patent for this invention.	[56,64]
1948	Ewald Arno Zdansky was the innovator behind the first pressurized industrial electrolyser, developed for the Swiss group Lonza.	[64–66]
1951	The German company Lurgi commercialized the initial high-pressure electrolyser (30 bars), having acquired the patent from Lonza.	[66,67]
1966	The first solid polymer electrolyte system (SPE) was developed by General Electric.	[55,56]

In 1900, Walther Hermann Nernst made a fundamental contribution to the development of the high-temperature–chemical thermodynamical relationship, which allowed for the calculation of a reduction potential of a reaction and the electrolyte YSZ, based on zirconium dioxide (ZrO_2) stabilized by yttrium oxide (Y_2O_3) [68]. The groundwork for high-temperature electrolysers and batteries was laid. However, it was only in the 1960s that NASA began developing high-temperature electrolysers as part of its space programmes [56].

One of the earliest publications concerning the description of high-temperature electrolysis for hydrogen production as a "future energy carrier" was written by W. Doenitz et al. [15] in 1980. The requirements for electrolyser electrodes, electrolyte, and interconnecting material were described. The experiment of water steam electrolysis was also performed at operational conditions T = 900 °C and p = 20 bar. The obtained operational curve is presented in Figure 8.

Also, the authors proposed to couple the electrolysis with the high-temperature reactor steam-generating process and, based on the HOT ELLY project [69], estimated the efficiency increase from 36–42% up to 44–51.5%.

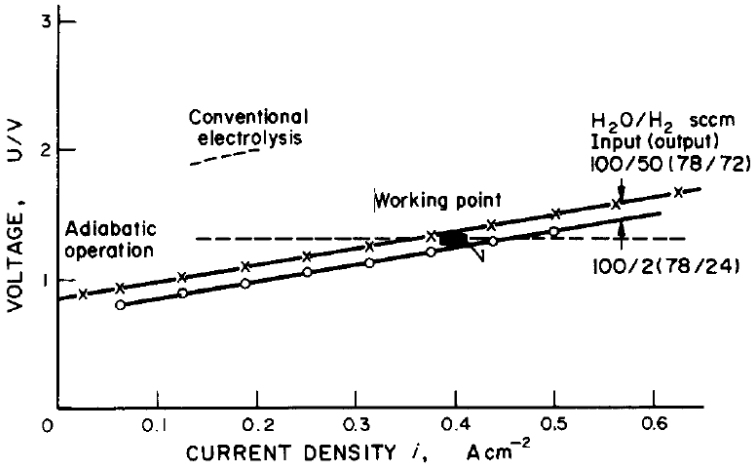


Figure 8. Cell characteristics and working point of high-temperature electrolysis operation [15].

Starting from the 1960s, NASA was developing the Advanced Life Support System, mainly for oxygen production from metabolically formed carbon dioxide and water [14,70–73]. The system consisted of twenty oxygen production stacks, six palladium tubes for hydrogen removal, a base plate, and housing (Figure 9). The approach to oxygen regeneration was developed by Westinghouse, and the idea was described by Elikan L. [13].

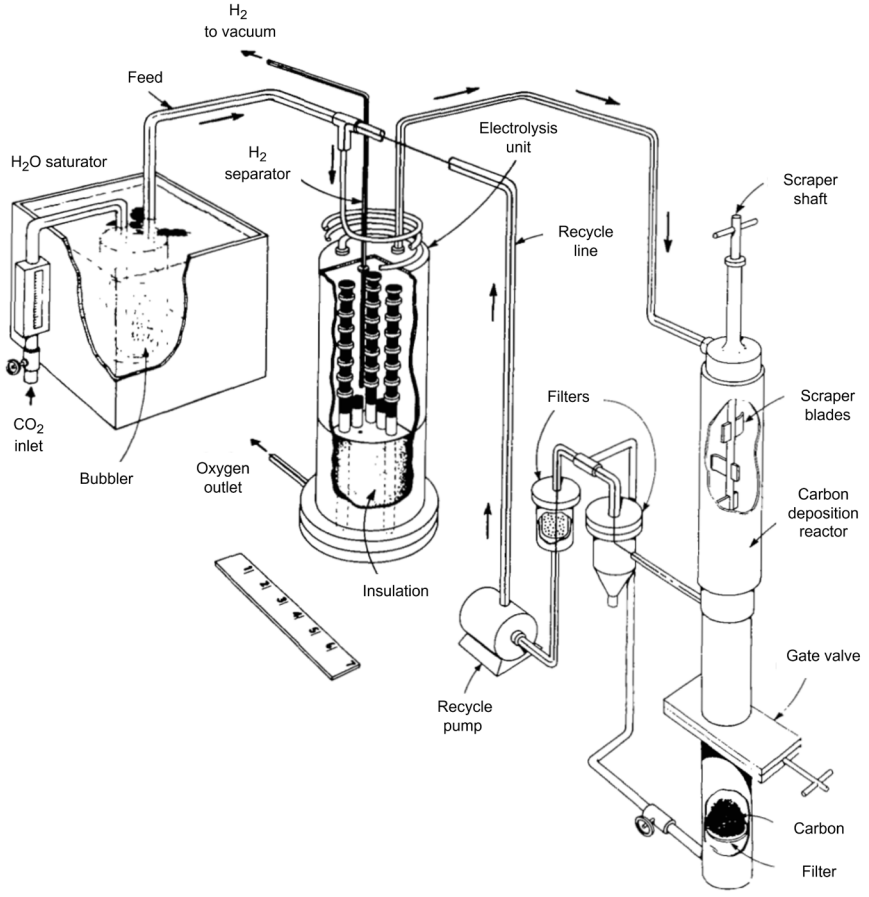


Figure 9. NASA system for oxygen production.

High-temperature electrolysis could be a valuable solution for long-term missions for the human exploration of Mars, providing the in situ resource utilization (ISRU): the majority of CO_2 in Mars' atmosphere could be turned into propellant and life support

consumables. The experimental studies of carbon dioxide electrolysis were provided by NASA and described by Tao G. [18,19].

Generally, the water steam and/or carbon dioxide high-temperature electrolysis began development as a technology for space programmes. However, further research and investigations showed that the high-temperature electrolysis is a promising solution for power and industrial sectors as the product is a syngas (H_2 + CO). Research organizations from numerous nations and regions are performing studies focused on creating novel materials, improving the durability and performance of stacks, and lowering the cost of syngas production since the turn of the century.

6. Conclusions

This manuscript has comprehensively addressed the technological evolution and potential of solid oxide electrolysis (SOE), co-electrolysis, and methanation as pivotal technologies for advancing the EU's climate neutrality objectives by 2050. Through historical analysis and detailed review of current technological capabilities, it is evident that SOE technologies, particularly when integrated with carbon capture and utilization strategies, offer a promising pathway for the decarbonization of the energy sector. The high efficiencies and capability of operating at elevated temperatures make SOEs particularly suitable for sustainable hydrogen production and power generation.

Co-electrolysis of steam and carbon dioxide has been highlighted as a significant advancement, facilitating syngas production that can be effectively integrated into existing industrial processes, thereby enhancing the versatility of renewable energy systems. The methanation process, catalytically converting carbon oxides and hydrogen into methane, provides a viable solution for energy storage and grid stabilization, which are critical for managing the intermittent nature of renewable energy sources.

The need for ongoing research and development is crucial, as evidenced by the discussion of system designs and operational enhancements that continue to push the boundaries of what is possible with SOE technologies. Future studies should focus on improving the durability and cost-effectiveness of these systems to facilitate wider adoption and implementation.

In conclusion, the integration of solid oxide electrolysis technologies within the renewable energy landscape represents a transformative approach towards achieving a sustainable and carbon-neutral energy future. However, integrating SOE/co-SOE and methanation systems with renewable energy sources like solar and wind faces challenges due to fluctuating power supply. The intermittency of renewable energy requires systems to operate flexibly under varying loads. SOE systems, though highly efficient, encounter thermal and mechanical stress from power variability, complicating the maintenance of their optimal operating temperatures (650–900 °C). Methanation reactors, reliant on the exothermic Sabatier reaction, are similarly sensitive to temperature fluctuations, risking reduced efficiency and catalyst deactivation. Effective integration demands robust energy and thermal storage solutions, hydrogen buffering, and advanced control systems for real-time synchronization. Addressing these challenges with material innovations and system optimization is crucial for reliable renewable energy coupling.

Funding: A part of research was funded by the Warsaw University of Technology within the Excellence Initiative: Research University (IDUB) programme (agreement nr 1820/92/Z01/2023). The authors are grateful for the research foundation of project WPC3/IMPRESSION/130/2023, supported by the National Centre for Research and Development (Poland) and the Ministry of Science and Technology (China).

Conflicts of Interest: The authors declare no conflict of interest.

References

1. European Comission. *A European Green Deal*; European Comission: Brussels, Belgium, 2020.
2. European Comission. *REPowerEU Plan*; European Comission: Brussels, Belgium, 2024.
3. Braack, M.K.; Milewski, N.; Trappe, H. Crossing Social Boundaries in an Immigration Context: Exogamy and Gendered Employment Patterns in Unions in Germany. *Gender Issues* **2022**, *39*, 142–176.
4. Kupecki, J.; Motylinski, K.; Jagielski, S.; Wierzbicki, M.; Brouwer, J.; Naumovich, Y.; Skrzypkiewicz, M. Energy Analysis of a 10 KW-Class Power-to-Gas System Based on a Solid Oxide Electrolyzer (SOE). *Energy Convers. Manag.* **2019**, *199*, 111934.
5. Milewski, J.; Kupecki, J.; Szczęśniak, A.; Uzunow, N. Hydrogen Production in Solid Oxide Electrolyzers Coupled with Nuclear Reactors. *Int. J. Hydrog. Energy* **2020**, *46*, 35765–35776. https://doi.org/10.1016/j.ijhydene.2020.11.217.
6. Eric, T.; Tony, W.; Casey, B.; Micah, C.; Michael, P.; Mark, R.; Randy, P. *Solid Oxide Based Electrolysis and Stack Technology with Ultra-High Electrolysis Current Density (>3 A/Cm²) and Efficiency*; A FuelCell Energy Company: Torrington, CT, USA, 2018.
7. Ebbesen, S.D.; Graves, C.; Mogensen, M. Production of Synthetic Fuels by Co-Electrolysis of Steam and Carbon Dioxide. *Int. J. Green Energy* **2009**, *6*, 646–660. https://doi.org/10.1080/15435070903372577.
8. Omojola, K. High Temperature Co Electrolysis of Carbon Dioxide and Steam in a Solid Oxide Cell for Synthesis Gas Production. Ph.D. Thesis, The University of Sheffield, Sheffield, UK, 2015.
9. Chen, M.; Høgh, J.V.T.; Nielsen, J.U.; Bentzen, J.J.; Ebbesen, S.D.; Hendriksen, P.V. High Temperature Co-Electrolysis of Steam and CO_2 in an SOC Stack: Performance and Durability. *Fuel Cells* **2013**, *13*, 638–645. https://doi.org/10.1002/fuce.201200169.
10. Wang, Y.; Liu, T.; Lei, L.; Chen, F. High Temperature Solid Oxide H_2O/CO_2 Co-Electrolysis for Syngas Production. *Fuel Process. Technol.* **2017**, *161*, 248–258. https://doi.org/10.1016/j.fuproc.2016.08.009.
11. Zheng, Y.; Wang, J.; Yu, B.; Zhang, W.; Chen, J.; Qiao, J.; Zhang, J. A Review of High Temperature Co-Electrolysis of H_2O and CO_2 to Produce Sustainable Fuels Using Solid Oxide Electrolysis Cells (SOECs): Advanced Materials and Technology. *Chem. Soc. Rev.* **2017**, *46*, 1427–1463.
12. Milewski, J.; Podhurska, V.; Martsinchyk, A.; Vasyliv, B.; Dybinski, O. Experimental and Theoretical Investigation of Contact Resistance in Molten Carbonate Fuel Cells. *J. Power Sources* **2023**, *568*, 232952. https://doi.org/10.1016/j.jpowsour.2023.232952.
13. Elikan, L.; Morris, J.P.; Wu, C.K. *Development of a Solid Electrolyte Carbon Dioxide and Water Reduction System for Oxygen Recovery*; NTRS: Chicago, IL, USA, 1972.
14. Weissbart, J.; Smart, W.H. Study of Electrolytic Dissociation of CO_2-H_2O Using a Solid Oxide Electrolyte. NASA CR-680. In *NASA Contractor Report*; NASA CR: Washington, DC, USA, 1967; pp. 1–92.
15. Doenitz, W.; Schmidberger, R.; Steinheil, E.; Streicher, R. Hydrogen Production by High Temperature Electrolysis of Water Vapour. *Int. J. Hydrogen Energy* **1980**, *5*, 55–63. https://doi.org/10.1016/0360-3199(80)90114-7.
16. Dönitz, W.; Erdle, E. High-Temperature Electrolysis of Water Vapor—Status of Development and Perspectives for Application. *Int. J. Hydrogen Energy* **1985**, *10*, 291–295. https://doi.org/10.1016/0360-3199(85)90181-8.
17. Isenberg, A. Energy Conversion via Solid Oxide Electrolyte Electrochemical Cells at High Temperatures. *Solid State Ion.* **1981**, *3–4*, 431–437. https://doi.org/10.1016/0167-2738(81)90127-2.
18. Tao, G. Study of Carbon Dioxide Electrolysis at Electrode/Electrolyte Interface: Part I. Pt/YSZ Interface. *Solid State Ion.* **2004**, *175*, 615–619. https://doi.org/10.1016/j.ssi.2004.01.077.
19. Tao, G. Study of Carbon Dioxide Electrolysis at Electrode/Electrolyte Interface: Part II. Pt-YSZ Cermet/YSZ Interface. *Solid State Ion.* **2004**, *175*, 621–624. https://doi.org/10.1016/j.ssi.2004.02.075.
20. Ebbesen, S.D.; Høgh, J.; Nielsen, K.A.; Nielsen, J.U.; Mogensen, M. Durable SOC Stacks for Production of Hydrogen and Synthesis Gas by High Temperature Electrolysis. *Int. J. Hydrogen Energy* **2011**, *36*, 7363–7373. https://doi.org/10.1016/j.ijhydene.2011.03.130.
21. Ebbesen, S.D.; Knibbe, R.; Mogensen, M. Co-Electrolysis of Steam and Carbon Dioxide in Solid Oxide Cells. *J. Electrochem. Soc.* **2012**, *159*, F482–F489. https://doi.org/10.1149/2.076208jes.
22. Ebbesen, S.D.; Jensen, S.H.; Hauch, A.; Mogensen, M.B. High Temperature Electrolysis in Alkaline Cells, Solid Proton Conducting Cells, and Solid Oxide Cells. *Chem. Rev.* **2014**, *114*, 10697–10734.
23. Morgenthaler, S.; Kuckshinrichs, W.; Witthaut, D. Optimal System Layout and Locations for Fully Renewable High Temperature Co-Electrolysis. *Appl. Energy* **2020**, *260*, 114218. https://doi.org/10.1016/j.apenergy.2019.114218.
24. Schreiber, A.; Peschel, A.; Hentschel, B.; Zapp, P. Life Cycle Assessment of Power-to-Syngas: Comparing High Temperature Co-Electrolysis and Steam Methane Reforming. *Front. Energy Res.* **2020**, *8*, 287. https://doi.org/10.3389/fenrg.2020.533850.
25. Bocanegra-Bernal, M.H.; de la Torre, S.D. Phase Transitions in Zirconium Dioxide and Related Materials for High Performance Engineering Ceramics. *J. Mater. Sci.* **2002**, *37*, 4947–4971.
26. Laguna-Bercero, M.A. Recent Advances in High Temperature Electrolysis Using Solid Oxide Fuel Cells: A Review. *J. Power Sources* **2012**, *203*, 4–16.
27. Yue, X.; Yan, A.; Zhang, M.; Liu, L.; Dong, Y.; Cheng, M. Investigation on Scandium-Doped Manganate La0.8Sr0.2Mn1-XScxO3-Cathode for Intermediate Temperature Solid Oxide Fuel Cells. *J. Power Sources* **2008**, *185*, 691–697.
28. Ai, N.; Li, N.; He, S.; Cheng, Y.; Saunders, M.; Chen, K.; Zhang, T.; Jiang, S.P. Highly Active and Stable $Er_{0.4}Bi_{1.6}O_3$ Decorated $La_{0.76}Sr_{0.19}MnO_{3+\delta}$ Nanostructured Oxygen Electrodes for Reversible Solid Oxide Cells. *J. Mater. Chem. A* **2017**, *5*, 12149–12157. https://doi.org/10.1039/c7ta02950k.
29. Chauveau, F.; Mougin, J.; Bassat, J.M.; Mauvy, F.; Grenier, J.C. A new anode material for solid oxide electrolyser: The neodymium nickelate $Nd_2NiO_{4+\delta}$. *J. Power Sources* **2010**, *195*, 744–749. https://doi.org/10.1016/j.jpowsour.2009.08.003.

30. Martsinchyk, A.; Szczęśniak, A.; Martsinchyk, K.; Dybiński, O.; Cinti, G.; Milewski, J.; Shuhayeu, P.; Łazor, M.; Ćwieka, K.; Skibiński, J.; et al. Molten Carbonate Electrolyzer for Synthetic Fuel Generation. *J. Power Sources* **2025**, *628*, 235741. https://doi.org/10.1016/j.jpowsour.2024.235741.
31. Bustamante, F.; Enick, R.M.; Cugini, A.V.; Killmeyer, R.P.; Howard, B.H.; Rothenberger, K.S.; Ciocco, M.V.; Morreale, B.D.; Chattopadhyay, S.; Shi, S. High-Temperature Kinetics of the Homogeneous Reverse Water–Gas Shift Reaction. *AIChE J.* **2004**, *50*, 1028–1041. https://doi.org/10.1002/aic.10099.
32. Pekridis, G.; Kalimeri, K.; Kaklidis, N.; Vakouftsi, E.; Iliopoulou, E.F.; Athanasiou, C.; Marnellos, G.E. Study of the Reverse Water Gas Shift (RWGS) Reaction over Pt in a Solid Oxide Fuel Cell (SOFC) Operating under Open and Closed-Circuit Conditions. *Catal. Today* **2007**, *127*, 337–346. https://doi.org/10.1016/j.cattod.2007.05.026.
33. Sun, Q.; Liu, C.-W.; Pan, W.; Zhu, Q.-M.; Deng, J.-F. In Situ IR Studies on the Mechanism of Methanol Synthesis over an Ultrafine Cu/ZnO/Al_2O_3 Catalyst. *Appl. Catal. A Gen.* **1998**, *171*, 301–308. https://doi.org/10.1016/S0926-860X(98)00096-9.
34. Zhao, K.; Bkour, Q.; Hou, X.; Kang, S.W.; Park, J.C.; Norton, M.G.; Yang, J.-I.; Ha, S. Reverse Water Gas Shift Reaction over CuFe/Al_2O_3 Catalyst in Solid Oxide Electrolysis Cell. *Chem. Eng. J.* **2018**, *336*, 20–27. https://doi.org/10.1016/j.cej.2017.11.028.
35. Wang, L.; Liu, H.; Liu, Y.; Chen, Y.; Yang, S. Effect of Precipitants on Ni-CeO2 Catalysts Prepared by a Co-Precipitation Method for the Reverse Water-Gas Shift Reaction. *J. Rare Earths* **2013**, *31*, 969–974. https://doi.org/10.1016/S1002-0721(13)60014-9.
36. Choi, S.; Sang, B.-I.; Hong, J.; Yoon, K.J.; Son, J.-W.; Lee, J.-H.; Kim, B.-K.; Kim, H. Catalytic Behavior of Metal Catalysts in High-Temperature RWGS Reaction: In-Situ FT-IR Experiments and First-Principles Calculations. *Sci. Rep.* **2017**, *7*, 41207. https://doi.org/10.1038/srep41207.
37. Bogolowski, N.; Sánchez Batalla, B.; Shin, B.; Drillet, J.-F. Activity of $La_{0.75}Sr_{0.25}Cr_{0.5}Mn_{0.5}O_{3-\delta}$, Ni_3Sn_2 and Gd-doped CeO_2 towards the reverse water-gas shift reaction and carburisation for a high-temperature H_2O/CO_2 co-electrolysis. *RSC Adv.* **2020**, *10*, 10285–10296. https://doi.org/10.1039/D0RA00362J.
38. Sabatier, P.; Senderens, J.B. New Methane Synthesis. *C. R. Acad. Sci. Paris* **1902**, *134*, 514–516.
39. Sun, D.; Simakov, D.S.A. Thermal management of a Sabatier reactor for CO_2 conversion into CH_4: Simulation-based analysis. *J. CO_2 Util.* **2017**, *21*, 368–382. https://doi.org/10.1016/j.jcou.2017.07.015.
40. Held, M.; Schollenberger, D.; Sauerschell, S.; Bajohr, S.; Kolb, T. Power-to-Gas: CO_2 Methanation Concepts for SNG Production at the Engler-Bunte-Institut. *Chem. Ing. Tech.* **2020**, *92*, 595–602. https://doi.org/10.1002/cite.201900181.
41. Schweitzer, J.M.; Viguié, J.C. Reactor Modeling of a Slurry Bubble Column for Fischer-Tropsch Synthesis. *Oil Gas Sci. Technol. Rev. De L'IFP* **2009**, *64*, 63–77. https://doi.org/10.2516/ogst/2009003.
42. Mebrahtu, C.; Krebs, F.; Abate, S.; Perathoner, S.; Centi, G.; Palkovits, R. CO_2 Methanation: Principles and Challenges. In *Studies in Surface Science and Catalysis*; Elsevier: Amsterdam, The Netherlands, 2019; pp. 85–103.
43. Medsforth, S. CLXIX.—Promotion of Catalytic Reactions. Part I. *J. Chem. Soc. Trans.* **1923**, *123*, 1452–1469. https://doi.org/10.1039/ct9232301452.
44. Pichler, H. Accounting in Hydrogenation. 1943. Avaliable online: https://www.osti.gov/biblio/6675880 (accessed on 15 September 2024)
45. Choe, S.J.; Kang, H.J. Adsorbed Carbon Formation and Carbon Hydrogenation for CO_2 Methanation on the Ni(111) Surface: ASED-MO Study. *Korean Chem. Soc.* **2005**, *26*, 1682–1688.
46. Martsinchyk, A. *Using MCFC for Capturing CO_2 from Flue Gases and Delivering to Sabatier Reactor for SNG Synthesis*; Institute of Heat Engineering (IHE), Warsaw, Poland, 2020.
47. Jiajian, G.; Wang, Y.; Ping, Y.; Hu, D.; Xu, G.; Gu, F.; Su, F. A Thermodynamic Analysis of Methanation Reactions of Carbon Oxides for the Production of Synthetic Natural Gas. *RSC Adv.* **2012**, *2*, 2358–2368. https://doi.org/10.1039/C2RA00632D.
48. Stangeland, K.; Kalai, D.; Li, H.; Yu, Z. CO_2 Methanation: The Effect of Catalysts and Reaction Conditions. *Energy Procedia* **2017**, *105*, 2022–2027. https://doi.org/10.1016/j.egypro.2017.03.577.
49. Martsinchyk, K.; Martsinchyk, A.; Łazor, M.; Shuhayeu, P.; Kupecki, J.; Niemczyk, A.; Błesznowski, M.; Milewski, J. Feasibility Study and Techno-Economic Assessment of Power-to-Gas (P2G) Technology Based on Solid Oxide Electrolysis (SOE). *J. Environ. Manag.* **2024**, *354*, 120425. https://doi.org/10.1016/j.jenvman.2024.120425.
50. Van Troostwijk, A.P.; Deiman, J.R. Sur Une Manière de Décomposer l'Eau En Air Inflammable et En Air Vital. *Obs. Phys.* **1789**, *35*, 369–378.
51. Paets van Troostwijk, A.; Deiman, J.R. Über Die Zerlegungdes Wassers in Brennbare Und Lebensluft Durch Denelektrischen Funken. *Ann. Phys.* **1790**, *2*, 130–141.
52. Troostwijk, P.A. Schets Der Nieuwe Ontdekkingenomtrent Het Water. *Algem. Mag. Wetensch. Kunst Smaak* **1790**, *4*, 909–941.
53. Berg, H. Johann Wilhelm Ritter–The Founder of Scientific Electrochemistry. *Rev. Polarogr.* **2008**, *54*, 99–103.
54. Zhang, J.; Zhang, L.; Liu, H.; Sun, A.; Liu, R.-S. *Electrochemical Technologies for Energy Storage and Conversion, 2 Volume Set*; John Wiley & Sons: Hoboken, NJ, USA, 2011; Volume 1; ISBN 3527328696.
55. Kreuter, W.; Hofmann, H. Electrolysis: The Important Energy Transformer in a World of Sustainable Energy. *Int. J. Hydrog. Energy* **1998**, *23*, 661–666. https://doi.org/10.1016/S0360-3199(97)00109-2.
56. Péra, M.-C.; Hissel, D.; Gualous, H.; Turpin, C. *Electrochemical Components*; John Wiley & Sons, Inc.: Hoboken, NJ, USA, 2013.
57. Katz, E. Electrochemical Contributions: William Nicholson (1753–1815). *Electrochem. Sci. Adv.* **2021**, *1*, e2160003. https://doi.org/10.1002/elsa.202160003.
58. de Levie, R. The Electrolysis of Water. *J. Electroanal. Chem.* **1999**, *476*, 92–93. https://doi.org/10.1016/S0022-0728(99)00365-4.
59. Faraday, M. On Electrical Decomposition. *Philos. Trans. R. Soc.* **1834,** *124*, 77–122. https://doi.org/10.1098/rstl.1834.0008.

60. Zhou, R.E. How to Offer the Optimal Demonstration of the Electrolysis of Water. *J. Chem. Educ.* **1996**, *73*, 786. https://doi.org/10.1021/ed073p786
61. Hendricks, L.J.; Williams, J.T. Demonstration of Electrochemical Cell Properties by a Simple, Colorful Oxidation-Reduction Experiment. *Chem. Educ.* **1982**, *59*, 586–587. https://doi.org/10.1021/ed059p586
62. Shakhashiri, B.Z. *Chemical Demonstrations: A Handbook for Teachers of Chemistry*; University of Wisconsin Press: Madison, WI, USA, 1992.
63. Hugerat, M. New Inexpensive Apparatus for Electrolysis. *Chem. Educ. J.* **2008**, *11*, 11–19.
64. Borja, A.N. *Desarrollo de Un Sistema Modular de Reacción Para El Estudio de La Producción de Oxígeno e Hidrógeno a Partir de La Electrólisis Del Agua*; Benemérita Universidad Autónoma de Puebla: Puebla, Mexico, 2018.
65. N Guillet, P.M. *Hydrogen Production by Electrolysis*; U.S. Department of Energy: Washington, DC, USA, 2015.
66. Zdansky, E.A. Pressure Electrolyzers. U.S. Patent 2,717,872A, 19 September 1955.
67. Ansar, A.S.; Gago, A.S.; Razmjooei, F.; Reißner, R.; Xu, Z.; Friedrich, K.A. Chapter 5-Alkaline Electrolysis—Status and Prospects. In *Electrochemical Power Sources: Fundamentals, Systems, and Applications*, Smolinka, T., Garche, J., Eds.; Elsevier: Amsterdam, The Netherlands, 2022; pp. 165–198, ISBN 978-0-12-819424-9.
68. Funke, K. Solid State Ionics: From Michael Faraday to Green Energy-The European Dimension. *Sci. Technol. Adv. Mater.* **2013**, *14*, 43502. https://doi.org/10.1088/1468-6996/14/4/043502.
69. Doenitz, W. Hydrogen Production with HOT ELLY. *Dornier-Post* **1977**, *1*, 17–19.
70. Hamilton Standart Devision of Unated Aircraft Corporation. *Trade-off Study and Conceptual Design of Regenarative Advanced Life Support System (AILSS)-NASA-CR1458*; NASA: Washington, DC, USA, 1970.
71. Elikan, L.; Morris, J.P. *Solid Electrolyte System for Oxygen Regeneration. NASA CR-1359*; NASA: Washington, DC, USA, 1969.
72. Weissbart, J.; Smart, W.H. *A Two-Cell 8-Ampere CO_2-H_2O Solid Electrolyte Electrolyzer for Oxygen Production*; National Aeronautics and Space Administration AMES Research Center: Moffett Field, CA, USA, 1970.
73. Smart, W.; Weissbar, J. *A 127-Ampere CO_2-H_2O Solid Oxide Electrolyzer-Reactor System For Production of Oxygen*; Electrochemical Soc Inc.: Pennington, NJ, USA, 1970.

Disclaimer/Publisher's Note: The statements, opinions and data contained in all publications are solely those of the individual author(s) and contributor(s) and not of MDPI and/or the editor(s). MDPI and/or the editor(s) disclaim responsibility for any injury to people or property resulting from any ideas, methods, instructions or products referred to in the content.